

Experimental study on fatigue crack propagation of fiber metal laminates

Zonghong Xie ^{*1}, Fei Peng ^{1a} and Tianjiao Zhao ^{2b}

¹ School of Astronautics, Northwestern Polytechnical University, Xi'an, China

² AVIC the First Aircraft Institute, Xi'an, China

(Received February 02, 2014, Revised April 27, 2014, Accepted May 03, 2014)

Abstract. This study aimed to investigate the fatigue crack growth behavior of a kind of fiber metal laminates (FML) under four different stress levels. The FML specimen consists of three 2024-T3 aluminum alloy sheets and two layers of glass/epoxy composite lamina. Tensile-tensile cyclic fatigue tests were conducted on centrally notched specimen at four stress levels with various maximum values. A digital camera system was used to take photos of the propagating cracks on both sides of the specimens. Image processing software was adopted to accurately measure the length of the cracks on each photo. The test results show that: (1) a - N and da/dN - a curves of FML specimens can be divided into transient crack growth segment, steady state crack growth segment and accelerated crack growth segment; (2) compared to 2024-T3 aluminum alloy, the fatigue properties of FML are much better; (3) da/dN - ΔK curves of FML specimens can be divided into fatigue crack growth rate decrease segment and fatigue crack growth rate increase segment; (3) the maximum stress level has a large influence on a - N , da/dN - a and da/dN - ΔK curves of FML specimens; (4) the fatigue crack growth rate da/dN presents a nonlinear accelerated increasing trend to the maximum stress level; (5) the maximum stress level has an almost linear relationship with the stress intensity factor ΔK .

Keywords: fatigue; experimental study; fiber metal laminates; crack growth rate; stress intensity factor

1. Introduction

Fiber metal laminates (FML) was originally developed at Delft University of Technology in Netherlands, from the beginning of the 1980s (Vlot and Gunnink 2001). This is a new family of hybrid materials consisting of thin metal layers bonded together by fibers embedded in an adhesive. As a result of this build-up, fiber metal laminates possess a mixture of the characteristics of both metals and composite materials. Initial development led to the ARALL (aramid fiber reinforced aluminum laminates) (Khan *et al.* 2009) variant using aramid fibers, which was first applied on the C-17 military transport aircraft around 1988 (Vermeeren 2003). Since the introduction of ARALL, several other FMLs have been developed, such as GLARE (glass fiber reinforced aluminum laminates), CARALL (carbon fiber reinforced aluminum laminates) (Sinmazçelik *et al.* 2011) and

*Corresponding author, Professor, E-mail: xzhae@nwpu.edu.cn

^a M.E. Student, E-mail: pengfei_npu@yeah.net

^b Assistant Engineer, E-mail: zhaotianjiao8885@163.com

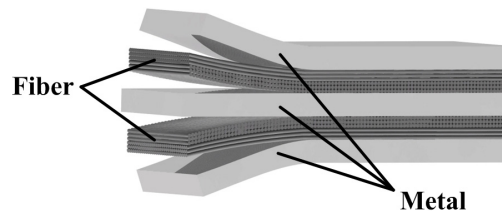


Fig. 1 The schematic figure of fiber metal laminates

TiGr (titanium-graphite hybrid laminates) (Buriánek *et al.* 2003). Each development was driven by the need for specific or enhanced properties with respect to the predecessors (Alderliesten 2005). An illustration of a typical cross-ply laminate is given in Fig. 1, where two cross-ply prepreg layers ($0^\circ/90^\circ$) are laminated between three metal layers.

FML possesses the inherited properties of an excellent machinability from aluminum alloys and both high strength and fatigue resistance from fiber reinforced composites. Experimental and theoretical researches have been performed on the fatigue crack propagation behavior study of GLARE (Chang and Yang 2008, Khan *et al.* 2011, Rans *et al.* 2011), which show that this new kind of hybrid material has excellent fatigue and damage tolerance properties due to the fiber bridging effect from the fatigue insensitive fibers imbedded. Compared to monolithic 2024-T3 aluminum alloy sheets, GLARE shows a considerably lower crack growth rate and a significant increase in the fatigue life under the same loading condition (Alderliesten and Homan 2006), but the threshold of GLARE is solely related to the fatigue threshold of the aluminum applied in the laminate (Alderliesten and Rans 2009). Due to its excellent fatigue crack growth properties, GLARE has reached its technology readiness with some aerospace applications, such as the cargo floor in the Boeing 777 in 1990, which is the first commercial application of a GLARE product. Large-scale application of GLARE was in 2001 when it was selected for the Airbus A380 jumbo jet (Vlot 2001). In addition to GLARE in the upper fuselage skin of the A380, it is also used in the A380 horizontal and vertical tail plane leading edges (Pitzer and Yang 2008). In 2008, the results of an experiment about two types of hybrid boron/glass/aluminum FMLs clearly showed that the fatigue crack initiation lives for both types of FMLs were superior to the monolithic aluminum alloy under the same loading condition (Chang *et al.* 2008). Therefore, it is quite worthwhile to experimentally study the fatigue crack propagation behavior of FML further and thoroughly to support the design and use of FML in near-term aerospace applications.

The main purpose of this experimental study is to investigate the fatigue crack propagation behavior of a kind of FML under four different cyclic loading conditions.

2. Fatigue crack propagation tests

2.1 Test specimens

The FML specimens used in this study are cross-ply laminates where two cross-ply glass/epoxy prepreg layers are laminated between three 2024-T3 aluminum alloy layers. The working area of the specimens is 200 mm long, 75 mm wide and the nominal thickness is 1.4 mm, as shown in Fig. 2. The thickness of each aluminum alloy layer is 0.254 mm. The layers of the FML specimens are

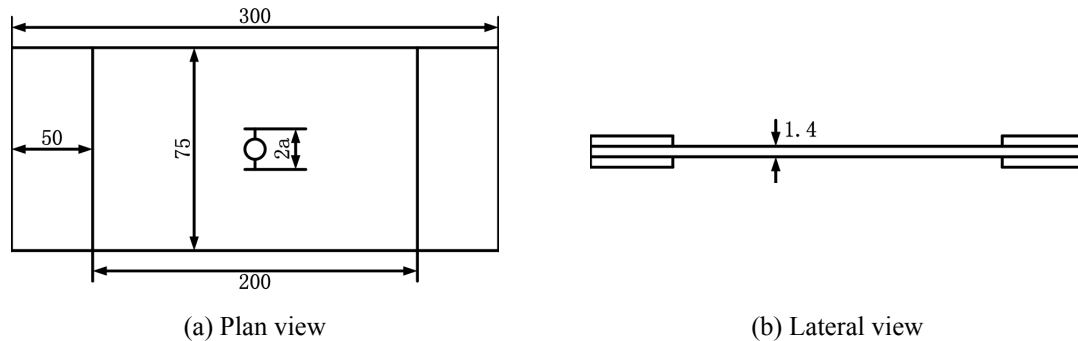


Fig. 2 Geometry and dimensions of the specimen (mm)

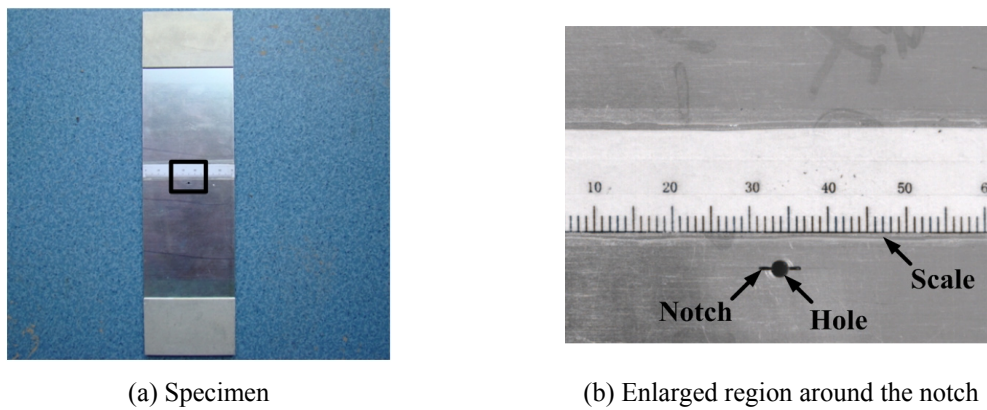


Fig. 3 Specimen and the enlarged region around the notch

[Al/0°/90°/Al/90°/0°/Al], and the 0° glass fiber layer is parallel to the loading direction. A notch with total length of $2a$ ($a = 2.5$ mm) is prefabricated at the center of the specimen by using laser beam. A picture of a test specimen is shown in Fig. 3(a) with an enlarged crack region shown in Fig. 3(b). There are total 12 specimens used in the test.

2.2 Experimental arrangement

The fatigue test was performed according to ASTM E647-95a by using a servo-hydraulic testing machine at room temperature under tension-tension cyclic loading with sinusoidal waves of frequency 10 Hz and stress ratio $R=0.1$. The loading direction was along the longitudinal direction of the test specimens, i.e., in the 0° fiber direction. The test used four kinds of nominal maximum stress level: S_{\max} from 100 MPa to 160 MPa with an increment of 20 MPa. Three FML specimens were tested for each maximum stress level. The test stopped when the crack propagated to the edge of specimens, or the number of loading cycles reached 1 million (the run-out number).

The fatigue crack propagation progress was recorded by a digital image system with two CCD cameras connected to the computer. The photos of propagating cracks on both sides of the specimen were taken in a regular interval manner of specified loading cycles. The photos were

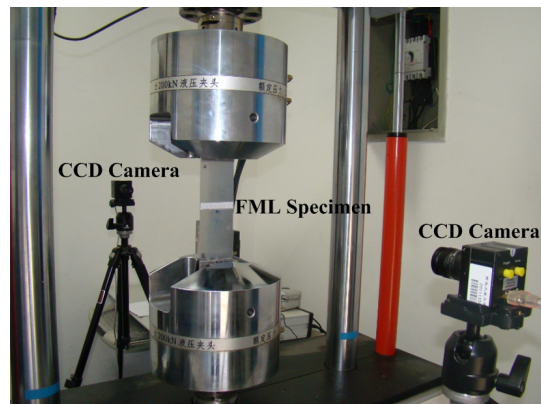


Fig. 4 Cameras and the specimen arrangement

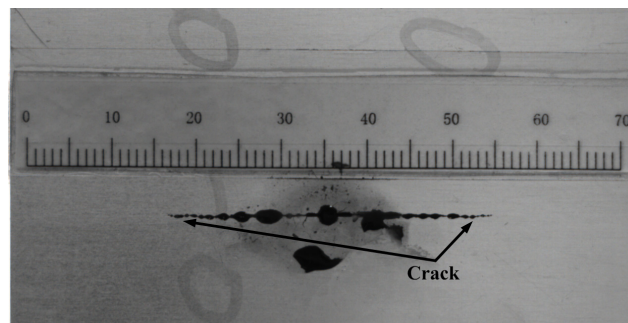


Fig. 5 Propagating cracks on one side of the specimen

saved in the computer for measurement and study afterwards by using image processing software called OPTPRO. This software can measure the crack length with accuracy within 0.1 mm. The testing and measuring systems are shown in Fig. 4.

2.3 Experimental phenomena

During the fatigue test, with an increase of loading cycles, the crack initiates at the tips of the prefabricated notch, and then propagates gradually along a direction perpendicular to the loading until it reaches the edge of the specimen, as shown in Fig. 5. After the test, one can see that the aluminum alloy layers of FML specimens under the loads of 120 MPa, 140 MPa and 160 MPa have been broken completely and some glass fibers are pulled out and broken. Fig. 6 shows the postmortem specimens for the fatigue test with four different maximum stress levels (100 MPa, 120 MPa, 140 MPa and 160 MPa).

2.4 Result analysis and discussion

2.4.1 a-N curves of the FML

Fig. 7 presents a series of a-N curves obtained by fatigue tests at various maximum stress levels

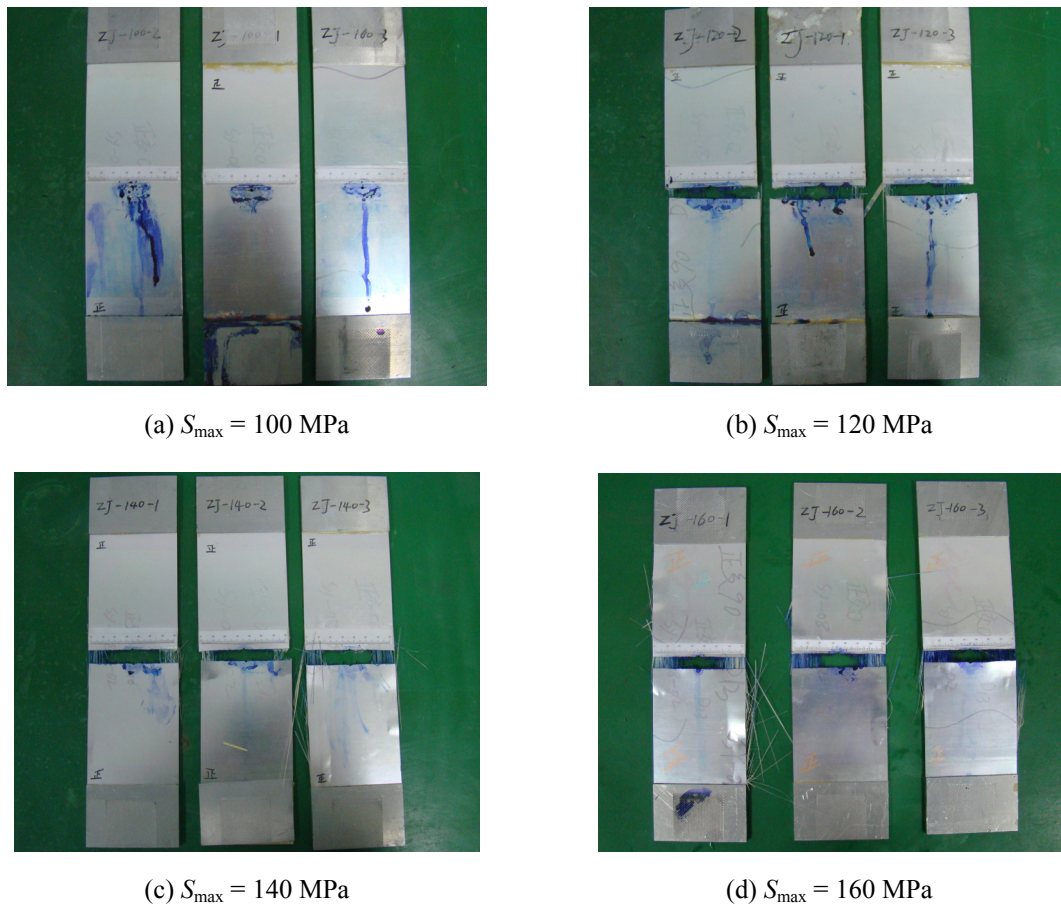


Fig. 6 The postmortem specimens for the fatigue test with different maximum stress levels

with $S_{\max} = 100$ MPa, 120 MPa, 140 MPa and 160 MPa. In order to ensure the accuracy and the universality of the test results, each figure gives the a-N curve of three specimens under the same maximum stress level.

The a-N curve, which is also called fatigue crack propagation curve, represents the relationship between the length of fatigue crack and the number of load cycles. For each test curve, one can see that a-N curves of FML specimens can be divided into three segments, as shown in Fig. 8: (1) transient crack growth segment; (2) steady state crack growth segment; and (3) accelerated crack growth segment.

In the transient crack growth segment, the fatigue crack propagation rate is relatively faster than in the steady state crack growth segment which is particularly evident when the maximum stress level is 100 MPa. This is due to the stiffness of the aluminum alloy is greater than the stiffness of the fibers in the FML specimens. Before the delamination of the FML, the stress acting on the aluminum alloy layers is greater than that on the glass fiber, and the tensile strength of aluminum alloy is smaller than that of the glass fiber.

The steady state crack growth segment is the longest in the whole fatigue life of FML. In the

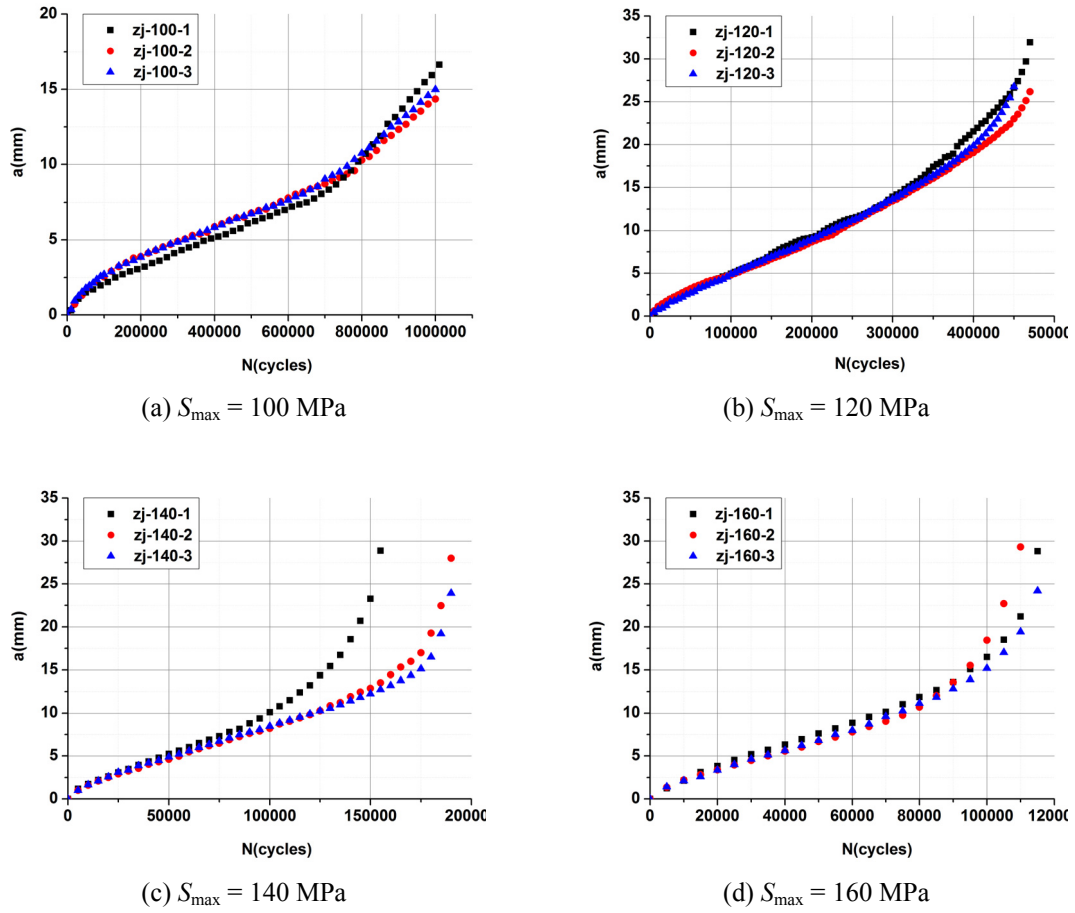


Fig. 7 a-N curves of specimens under four different maximum stress levels

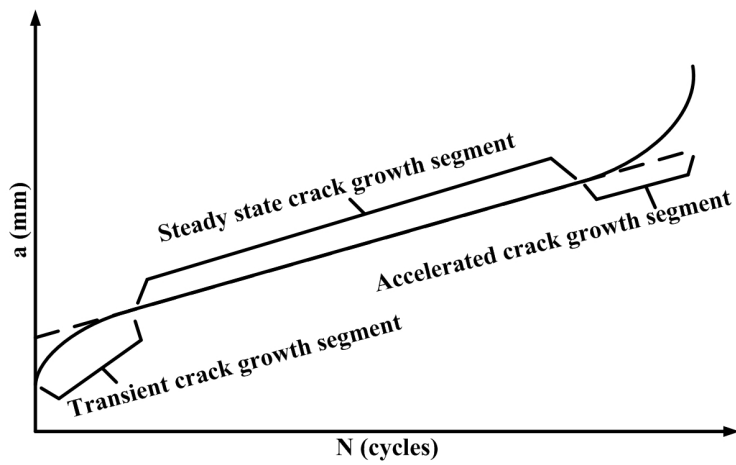


Fig. 8 Three segments of FML's a-N curve

steady state growth segment, the value of da/dN becomes stable, which means that the fatigue crack grows at a constant rate, independent of the crack length. In the dehiscence zone of the aluminum alloy layers, most of the stress is passed through the resin to the fiber which is insensitive to fatigue, and this process, i.e., the bridging effect of the fiber (Ma *et al.* 2014), inhibits the propagation of the crack. When the stress is transmitted through the resin layer, there will be producing a periodic shear stress in the resin layer, and this periodic shear stress induces the delamination between the aluminum alloy layers and the fiber layers. This delamination growth process to some extent reduces the stress of the fiber layer and alleviates the breakage of the fiber. In conclusion, the homeostasis between the crack propagation and the delamination growth contributes to the steady growth of the fatigue crack.

In the accelerated crack growth segment, because of the considerable reduction of the load bearing cross section area of the specimen, crack growth rate increases significantly. During this period, large numbers of fibers break inside the specimen, and the bridging effect declines sharply,

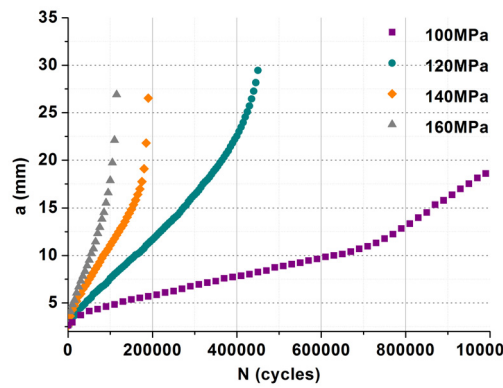


Fig. 9 Fatigue crack propagation curves under different loads

Table 1 The fatigue life of FML specimens

Specimen	S_{max}	Fatigue cycles ($\times 10^3$ cycles)	Average fatigue life ($\times 10^3$ cycles)
Zj-100-1	100MPa	1000	—
Zj-100-2		1000	
Zj-100-3		1000	
Zj-120-1	120MPa	470	465
Zj-120-2		470	
Zj-120-3		454	
Zj-140-1	140MPa	157	180
Zj-140-2		191	
Zj-140-3		192	
Zj-160-1	160MPa	118	117
Zj-160-2		113	
Zj-160-3		120	

which further increases the crack growth rate.

Comparing the a-N curves of the FML specimens under four maximum stress levels, as shown in Fig. 9, one can see that with the enhancement of the S_{\max} , the fatigue crack growth rate of the FML specimen increases rapidly, and the fatigue life reduces greatly. The fatigue life of all specimens is shown in Table 1.

As shown in Fig. 10, compared with 2024-T3 aluminum alloy, FML not only has a higher fatigue life, but also has a very excellent ability to inhibit crack propagation. With the propagation of the crack, the fatigue crack growth rate of 2024-T3 aluminum alloy indicates a significant exponential increase trend, which is distinct from the orthogonal FML. The crack propagation process of FML is divided into three stages, and the steady state crack growth segment occupies the most of the time of the crack propagation process. This is because that a fiber bridging mechanism at the crack tip dramatically reduced the rate of crack growth in FML specimens relative to the aluminum alloy specimen.

2.4.2 da/dN - a curves and da/dN - ΔK curves of the FML

According to the experiment data, the secant method, i.e., Eq. (1) was used to get the crack propagation rate under the four different maximum stress levels. And the da/dN - a curve could be drawn, as shown in Figs. 11(a)-14(a).

$$\frac{da}{dN} \cong \frac{\Delta a}{\Delta N} \quad (1)$$

To study the crack propagation rate further, Eq. (2) and cubic fit method were used to calculate ΔK and get the da/dN - ΔK curves, as shown in Fig. 11(b)-14(b). In Eq. (2), P_{\max} is the maximum load and P_{\min} is the minimum load. B is the thickness of the specimen and the W is the width of the specimen. The value of a is equal to the half length of the crack.

$$\begin{aligned} \Delta K &= \frac{\Delta P}{B} \left(\frac{\pi a}{2W} \sec \frac{\pi a}{2} \right)^{\frac{1}{2}} \\ \Delta P &= P_{\max} - P_{\min} \\ \alpha &= \frac{2a}{W} \end{aligned} \quad (2)$$

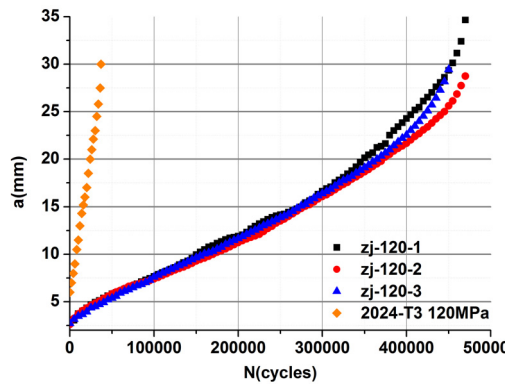


Fig. 10 $S_{\max} = 120$ MPa, a-N curves of 2024-T3 aluminum alloy and the FML

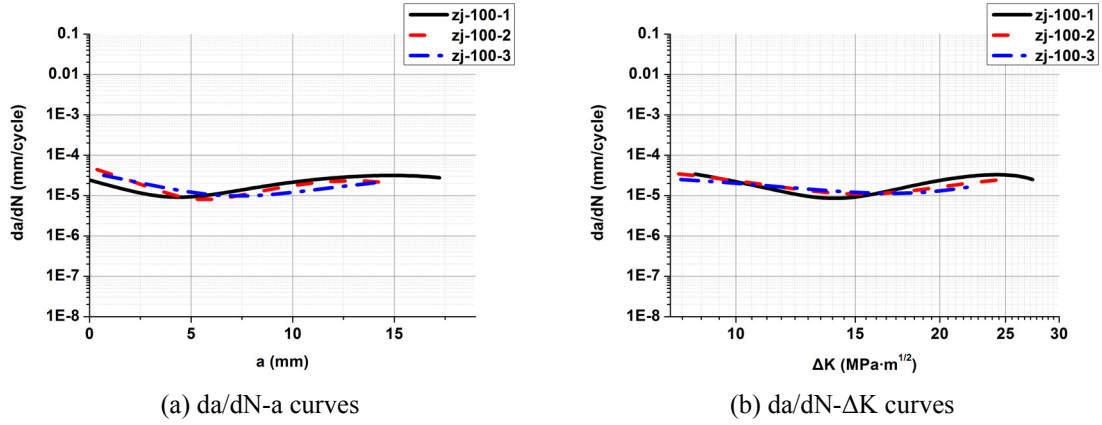


Fig. 11 da/dN - a and da/dN - ΔK curves of FML when $S_{max} = 100$ MPa

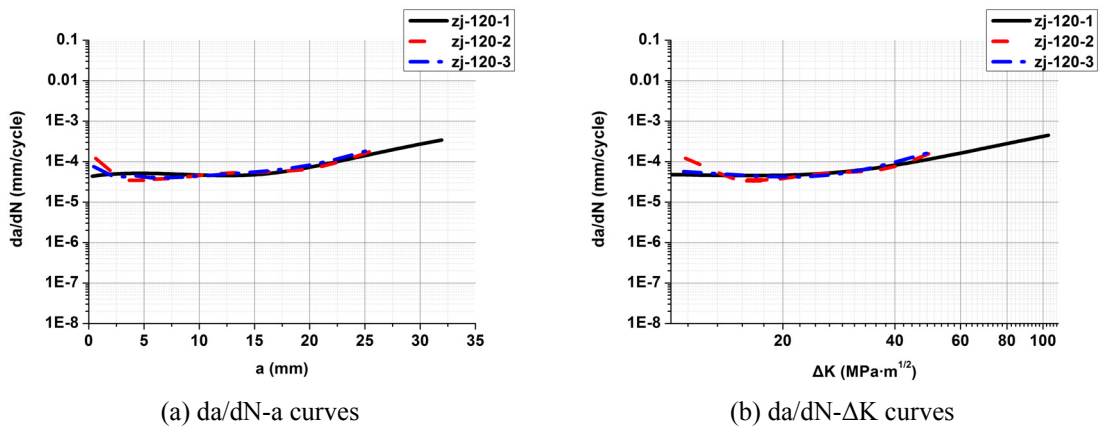


Fig. 12 da/dN - a and da/dN - ΔK curves of FML when $S_{max} = 120$ MPa

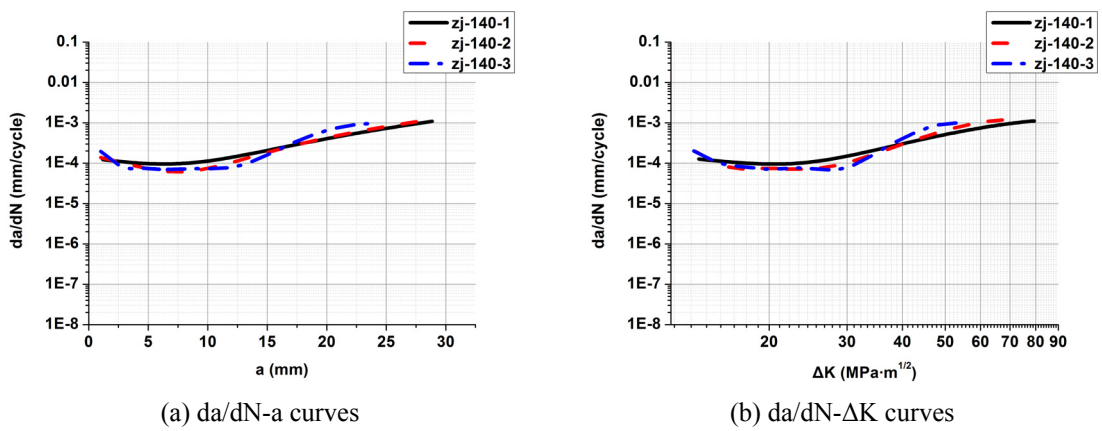


Fig. 13 da/dN - a and da/dN - ΔK curves of FML when $S_{max} = 140$ MPa

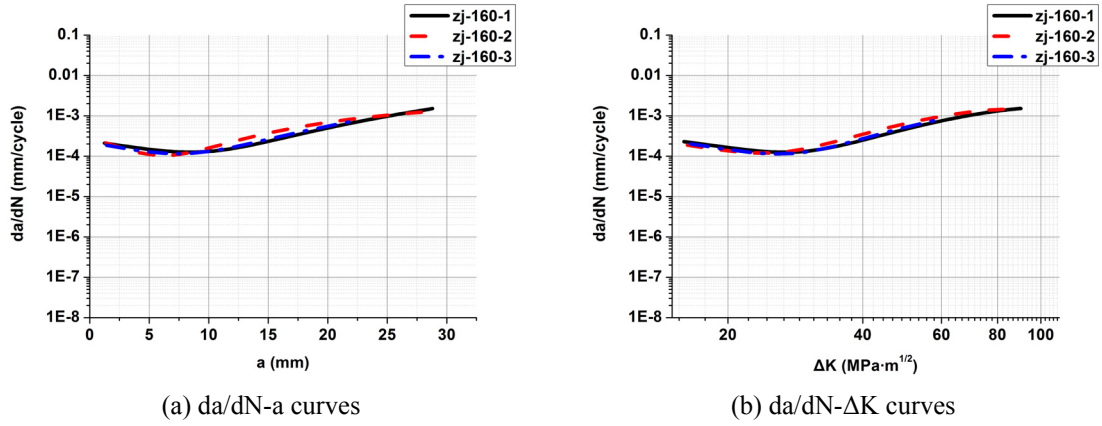


Fig. 14 da/dN - a and da/dN - ΔK curves of FML when $S_{\max} = 160$ MPa

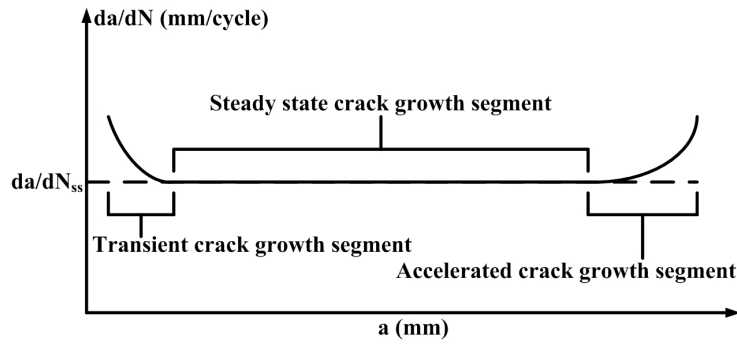


Fig. 15 Three segments of FML's da/dN - a curve

Table 2 da/dN_{ss} and da/dN_{\max} of accelerated crack growth segment under four different S_{\max}

S_{\max}	da/dN_{ss} (steady state crack growth segment)	da/dN_{\max} (accelerated crack growth segment)
100 MPa	1.0×10^{-5} mm/cycle	2.2×10^{-5} mm/cycle
120 MPa	4.0×10^{-5} mm/cycle	3.0×10^{-4} mm/cycle
140 MPa	8.0×10^{-5} mm/cycle	1.0×10^{-3} mm/cycle
160 MPa	1.0×10^{-4} mm/cycle	1.5×10^{-3} mm/cycle

For da/dN - a curves, one can see that each da/dN - a curve of FML can also be divided into three segments, as shown in Fig. 15: (1) transient crack growth segment; (2) steady state crack growth segment; and (3) accelerated crack growth segment. In the early stage of the crack growth, due to no fiber bridging effect, the crack growth of the orthogonal FML specimens is fast. With the increase of the crack length, bridging fibers begin to carry more loads from the aluminum layer, and the crack growth rate gradually slows and reaches a steady growth rate, not varying with the changes of the length of the crack. This rate is called steady state crack growth rate da/dN_{ss} , which

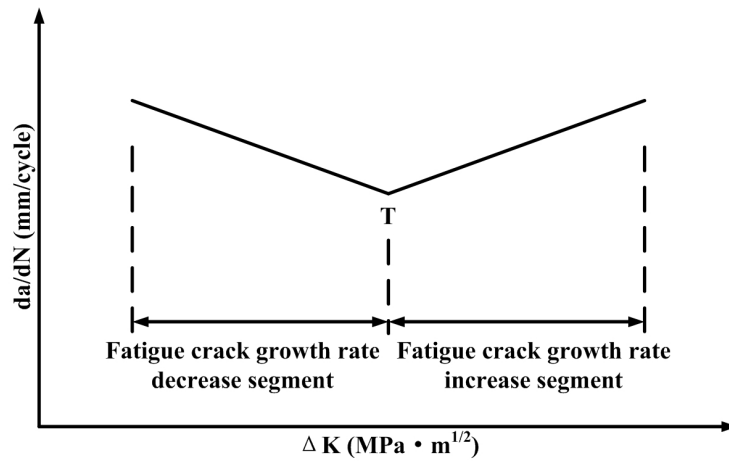


Fig. 16 Two segments of FML’s da/dN-ΔK curve

Table 3 ΔK and the length of the fatigue crack at the turning point T

S_{max}	ΔK	The length of the fatigue crack
100 MPa	15 MPa·m ^{1/2}	5.6 mm
120 MPa	19 MPa·m ^{1/2}	6.5 mm
140 MPa	23 MPa·m ^{1/2}	7.2 mm
160 MPa	28 MPa·m ^{1/2}	8.4 mm

is the function of the stress level. The independence of the da/dN_{ss} respect to the length of the crack indicates that once the relationship between the da/dN_{ss} and the load amplitude is ascertained, the crack of the laminates can be predicted based on the stress level, and not requiring any fracture mechanics analysis. The values of da/dN_{ss} and da/dN_{max} of the accelerated crack growth segment under four different maximum stress levels are shown in Table 2. With the rising of the stress level, da/dN_{ss} continues to increase and the steady state crack growth segment gradually shortens, and the da/dN in accelerated crack growth segment increases at the same time.

According to da/dN - ΔK curves, the value of da/dN initial decreases and then increases, and each curve can be divided into two stages: (1) fatigue crack growth rate decrease segment; and (2) fatigue crack growth rate increase segment, as shown in Fig. 16. The decline of the fatigue crack growth rate is mainly due to the bridging effect of the fibers. When da/dN - ΔK curves cross the turning point T , due to the delamination between the aluminum alloy layers and the fiber layers, the fiber bridging effect gradually weakens, leading to the value of da/dN increasing with the augment of the amplitude of the stress intensity factor ΔK . With the increase of the maximum stress level, both of ΔK and the length of the fatigue crack at the turning point become larger, as shown in Table 3.

According to Fig. 17, the maximum stress level has a large influence on both da/dN - a curves and da/dN - ΔK curves of FML specimens. At the same crack length, the crack growth rate increases when S_{max} increases, as shown in Fig. 17(a). In Fig. 17(b), the arrows and point A, B, C, and D indicate the turning point between the decreasing and increasing stage of da/dN - ΔK curves.

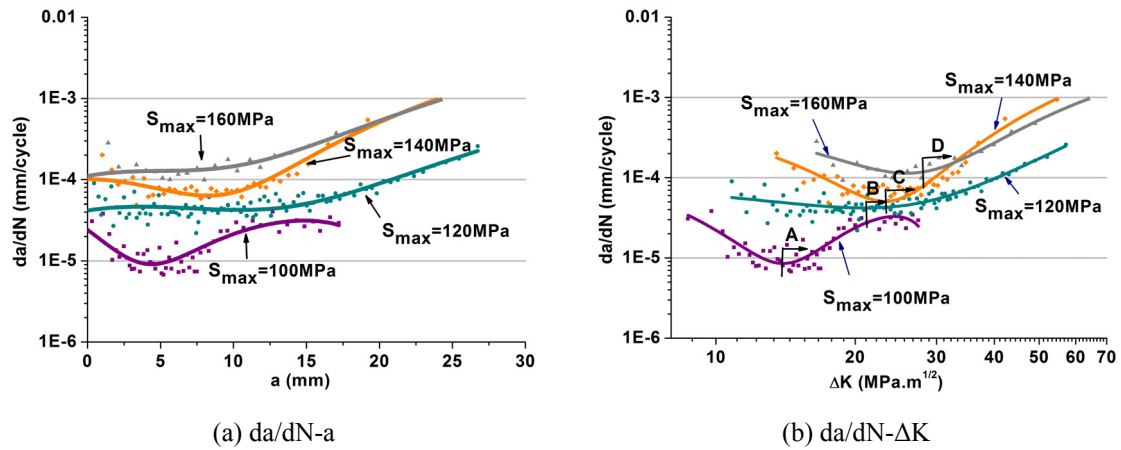


Fig. 17 da/dN - a and da/dN - ΔK curves of FML under four different loads

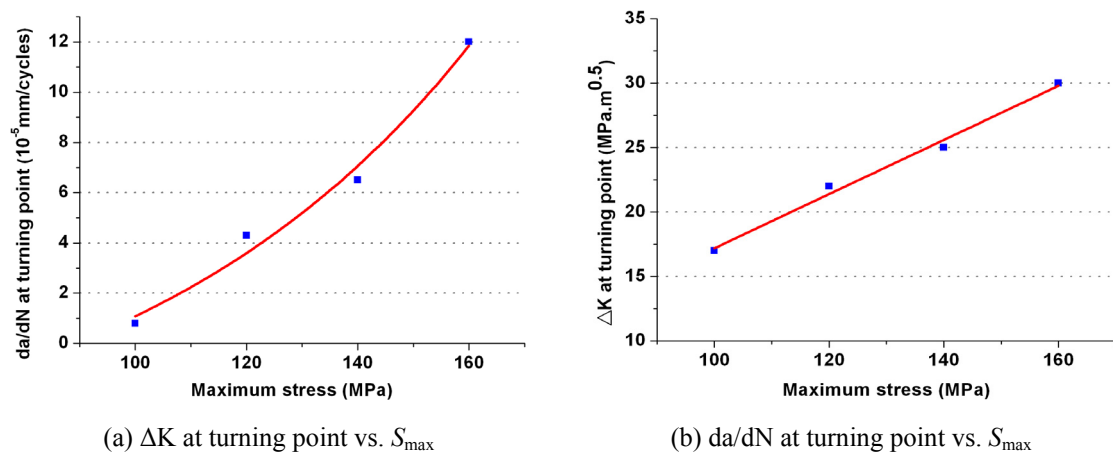


Fig. 18 The values of ΔK and da/dN at turning point vs. S_{max}

The turning point occurs at a smaller crack length as the maximum stress level increases.

In Fig. 18(a), the fatigue crack growth rate da/dN presents a nonlinear accelerated increasing trend to the maximum stress level. Fig. 18(b) shows that maximum stress level has an almost linear relationship with the stress intensity factor ΔK .

3. Conclusions

An experimental study has been carried out for researching the properties of fatigue crack propagation of fiber metal laminates. The conclusions of this study are as followed:

- The a - N and da/dN - a curves of FML specimens can be divided into three segments: (1) transient crack growth segment; (2) steady state crack growth segment; and (3) accelerated

crack growth segment.

- Compared to 2024-T3 aluminum alloy, because of a fiber bridging mechanism at the crack tip dramatically reducing the rate of crack growth in FML, FML not only has a higher fatigue life, but also has a very excellent ability to inhibit crack propagation.
- The cyclic loading value has a great influence on the fatigue crack growth rate and the fatigue life of the FML, and both of these two quantities increase with the enhancement of the stress level.
- The fatigue crack growth rate da/dN presents a nonlinear accelerated increasing trend to the maximum stress level.
- The maximum stress level has an almost linear relationship with the stress intensity factor ΔK .

References

- Alderliesten, R. (2005), *Fatigue Crack Propagation and Delamination Growth In Glare*, Delft University Press, Delft, South Holland, The Netherlands.
- Alderliesten, R.C. and Homan, J.J. (2006), "Fatigue and damage tolerance issues of Glare in aircraft structures", *Int. J. Fatigue*, **28**(10), 1116-1123.
- Alderliesten, R. and Rans, C. (2009), "The meaning of threshold fatigue in fibre metal laminates", *Int. J. Fatigue*, **31**(2), 213-222.
- Burianek, D.A., Giannakopoulos, A.E. and Spearing, S.M. (2003), "Modeling of facesheet crack growth in titanium-graphite hybrid laminates, part I", *Engng. Fract. Mech.*, **70**(6), 775-798.
- Chang, P.Y. and Yang, J.M. (2008), "Modeling of fatigue crack growth in notched fiber metal laminates", *Int. J. Fatigue*, **30**(12), 2165-2174.
- Chang, P.Y., Yeh, P.C. and Yang, J.M. (2008), "Fatigue crack initiation in hybrid boron/glass/aluminum fiber metal laminates", *Mater. Sci. Engng. A*, **496**(1), 273-280.
- Khan, S.U., Alderliesten, R.C. and Benedictus, R. (2009), "Post-stretching induced stress redistribution in fibre metal laminates for increased fatigue crack growth resistance", *Compos. Sci. Technol.*, **69**(3), 396-405.
- Khan, S.U., Alderliesten, R.C. and Benedictus, R. (2011), "Delamination in fiber metal laminates (GLARE) during fatigue crack growth under variable amplitude loading", *Int. J. Fatigue*, **33**(9), 1292-1303.
- Ma, Y., Xia, Z.C. and Xiong, X.F. (2014), "Fatigue crack growth in fiber-metal laminates", *Sci. China Phys., Mech. Astron.*, **57**(1), 83-89.
- Pitzer, C. and Yang, J.M. (2008), *Hybrid Metal Laminate (HML) Manufacturing Planning Evaluation and Assessment*, University of California, Los Angeles, CA, USA.
- Rans, C.D., Alderliesten, R.C. and Benedictus, R. (2011), "Predicting the influence of temperature on fatigue crack propagation in fibre metal laminates", *Engng. Fract. Mech.*, **78**(10), 2193-2201.
- Sinnmazçelik, T., Avcu, E., Bora, M.Ö. and Çoban, O. (2011), "A review: Fibre metal laminates, background, bonding types and applied test methods", *Mater. Des.*, **32**(7), 3671-3685.
- Vermeeren, C.A.J.R. (2003), "An historic overview of the development of fibre metal laminates", *Appl. Compos. Mater.*, **10**(4-5), 189-205.
- Vlot, A. (2001), *Glare: History of the Development of a New Aircraft Material*, Kluwer Academic Publishers, Dordrecht, South Holland, The Netherlands.
- Vlot, A. and Gunnink, J.W. (2001), *Fibre Metal Laminates: An Introduction*, Kluwer Academic Publishers, Dordrecht, South Holland, The Netherlands.